Flow past a row of trapezoidal tabs: experimental and numerical study

Charbel Habchi, Farid Khalil, Thierry Lemenand, Dominique Della Valle, Hassan Peerhossaini

Proceedings of ICFD11:
Eleventh International Conference of Fluid Dynamics
December 19-21, 2013, Alexandria, Egypt

ICFD11-EG-4070

Flow Past a Row of Trapezoidal Tabs: Experimental and Numerical Study

Charbel Habchi
ETF group
Lebanese International University
Beirut, Lebanon

Farid Khalil
ETF group
Lebanese International University
Beirut, Lebanon

Thierry Lemenand
LTN CNRS UMR 6607, LUNAM University
Nantes, France

Dominique Della Valle
ONIRIS
Nantes, France

Hassan Peerhossaini
LIED, University of Paris 7 Diderot
Paris, France

ABSTRACT
Trapezoidal mixing tabs are used to generate complex coherent structures: a counter-rotating vortex pair and hairpin like structures develop downstream the tab. The flow pattern of these vortical structures and their interaction has been analyzed and comprehended recently. Nevertheless, the individual contribution of these structures on turbulent mixing and micro mixing are not yet well understood, and remain important sake for the purpose of transfer intensification in industrial devices like the HEV mixer. The present study is a first attempt of analysis of these contributions, based on both experimental (LDV) and numerical approaches for the knowledge of the 3D flow structures.

KEYWORDS:
Longitudinal vortices; Hairpin-like structures; Trapezoidal tabs; Turbulent mixing; Multifunctional heat exchangers.

INTRODUCTION
Flow past trapezoidal mixing tabs has been extensively studied due to its capability to enhance turbulent mixing, mass transfer and phase dispersion [1-5] by the generation of coherent structures similar to those encountered in natural turbulent boundary layers. Gretta and Smith [1] identified two types of flow structures: a counter-rotating vortex pair (CVP) formed due to the pressure difference across the tab and a periodic sequence of hairpin-like structures (or horseshoe vortices) shed from the tab edges, riding the CVP and convecting downstream. The interactions of these structures with the main flow and between themselves greatly enhance mixing and mass exchange between low momentum near-wall region and high momentum zone in the free stream flow [1-5]. These tabs are widely used in the industry by simply mounting them on a pipe or channel wall. This is the case of the High Efficiency Vortex mixer (HEV) where several arrays of trapezoidal tabs produce a complex flow pattern due to the recombination of the streamwise vortices downstream by the following arrays in the confined flow. DNS study by Dong and Meng [3] for a flow past a trapezoidal tab showed that, while propagating downstream, the CVP goes on deforming and splitting into hairpin vortex legs due to the instability caused by the difference of vorticity magnitude in the vortex core and the surrounding fluid. Primary hairpins are then created and grow continuously as they convect downstream. Secondary instabilities can also occur to generate secondary hairpins and reversed vortices in the tab wake [2,3]. The growth of the hairpin strength was attributed to the ejection and entrainment of new vorticity from the near-wall local boundary layer toward the hairpin head, providing a self-sustained mechanism for the hairpin structures. The evolution and dynamics of these vortical structures and their interaction have been widely analyzed and comprehended [1-5]. However, the specific role of these structures on turbulent meso and micro mixing has not yet been explained. The present study is aimed to propose this analysis from the knowledge of the 3D flow structures. The mesomixing process, or turbulent transport at the scale of the large eddies, is analyzed from the Reynolds stress field. The micromixing is the homogenization at the molecular scale, and a determinant factor

for the sake of chemical reactions. It results from a scale reduction is the turbulent cascade till Kolmogorov scale, and continued by laminar stirring. As far as the mixing at Kolmogorov scale is "slower" and hence limiting, the micromixing efficiency is characterized by the turbulent kinetic energy dissipation ε, as a parameter scaling the Kolmogorov scale.

This paper is organized as follows: in section 2, experimental apparatus and measurement method are presented. Section 3 describes the numerical simulations procedure. Results and discussion are given in section 4. Section 5 is devoted for concluding remarks.

EXPERIMENTAL SETUP

Test section

The test section consists on a straight circular pipe of 20 mm inner diameter in which a row of four diametrically opposed mixing tabs are fixed (Figure 1 (a)). The tabs are inclined 30° with respect to the tube wall (Figure 1 (b)). The test section is preceded by a preconditioner (2000 mm straight Plexiglas pipe) to produce a fully developed turbulent flow at the test section inlet, and is followed by a postconditioner (200 mm straight Plexiglas pipe). Care was taken so the connections between the different elements do not disturb the flow. A safety valve is added to the circuit as well as a pulsation dumper to ensure stable flow in the test section. The temperature of the working fluid (water) is maintained constant at 298 K. The experiments are carried out in a turbulent flow with Reynolds numbers 7500, 10000, 12500 and 15000.

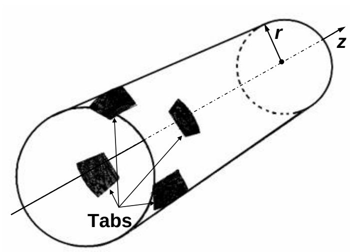

(a)

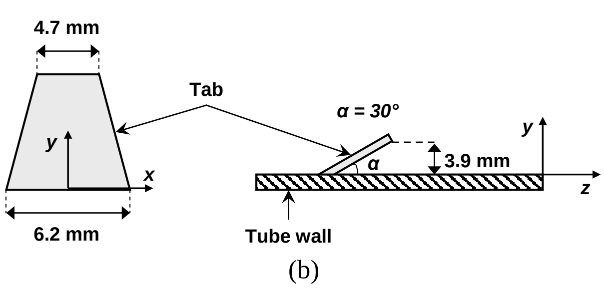

(b)

Figure 1. (a) Global view of the test section and (b) mixing tab dimensions

LDV measurements and data acquisition

The measurements are performed using a Dantec LDV system (Laser Doppler Velocimetry) equipped with a 10 W argon-ion laser source and two BSA-enhanced signal-processing units (57N20 BSA and 57N35 BSA enhanced models). A lens of 160 mm focal distance is used. A lightweight precision three-dimensional traversing mechanism controlled via PC is used to displace the measuring volume. The data-acquisition rate was 1-4 kHz and the sampling particle number was 30000. Measurements are taken on radial profiles in the center-plane of one mixing tab, at 3, 6, 10, 25 and 35 mm downstream from the tab tip.

To ensure the repeatability of LDV measurements, experiments were iterated four times for radial profiles at different positions for Reynolds number 15000. The relative standard deviation for the mean and RMS fluctuating velocities depends on the location of the measurement volume. It is maximal in the near-wall region, at low-velocity zone, and minimal in the flow core region. The global mean standard deviation is 6% for the mean velocities and 5% for the fluctuating velocities.

NUMERICAL PROCEDURE

Numerical method

In this study, a three dimensional numerical simulation of the heat transfer is carried out by using the CFD code Fluent®, to access the 3D flow mechanism in the studied geometry. The continuity equations for mass and momentum are solved sequentially with double precision, segregated and second-order accuracy. Pressure-velocity coupling is performed by finite volume with SIMPLE algorithm. The RSM [8-10] model is used in the present study to analyze the fluid dynamics and turbulent mixing process in a flow downstream from a row of trapezoidal mixing tabs. In this model the transport equations are solved for each term of the Reynolds stress tensor.

Boundary conditions

The description of the flow in the near-wall region is performed by using the "two layer model", where the Navier-Stokes equations are solved in the viscous sub-layer. No-slip boundary conditions are applied to the solid surface of the tabs and of the pipe wall. At the tabs array inlet a 1/7 power-law velocity profile is imposed, which corresponds to the theoretical velocity profile for fully turbulent developed flow in a pipe [11]. The turbulence kinetic energy and the dissipation rate are fixed by the intensity of turbulence I, derived from the empty tube equilibrium state [11].

Computational grid

By considering the symmetry of the mixer, the studied section is reduced to a sector of $\pi/8$. A non-uniform unstructured three-dimensional mesh with hexahedral volumes is adopted and refined at all solid boundaries. The refinement is necessary to resolve correctly the strong velocity and turbulence gradients in this region. To determine the appropriate density mesh, the solver is run for several mesh densities: the density mesh is increased until no effect on the results is detected. The criterion for the grid sensitivity test is based on velocity profiles and turbulence dissipation rate at 3 mm downstream from the tab tip. The mesh with lowest node density yielding high-quality results is used to simulate the flow in the studied geometry. The appropriate meshing contains 484,352 cells.

Convergence criterion

In order to determine an adequate convergence criterion, a series of simulations for different stop-criterion values ranging from 10^{-3} to 10^{-9} were carried out. Beyond a convergence criterion of 10^{-6}, no significant changes were observed in the velocity field or turbulence quantities; this latter value was hence retained as the convergence criterion.

Experimental validation

Numerical simulations are found to predict fairly the flow pattern in the studied test section. The overall relative standard deviation does not exceed 8%. It is maximal in the shear zone $(0.36 < y/R < 0.55)$, low velocities inducing less LDV precision, and minimal in the core region $(0.55 < y/R < 1)$, high velocities resulting good LDV precision.

RESULTS AND DISCUSSIONS

Flow structures effects on turbulent meso and micro mixing

The distribution of Reynolds shear stress $<u'v'>$, obtained from numerical simulations, is plotted in Figure 2 on two cross sections downstream from the tab. Black arrows on this figure are dimensioned by the velocity magnitude. From Figure 2 it is observed that the higher values of negative $<u'v'>$ coincide with the region occupied by the secondary hairpin legs. The other maximum values of positive $<u'v'>$ are observed in the region of primary hairpin legs with values lower than those of secondary hairpins. This suggests that the secondary and primary hairpin legs are the most contributing on mesomixing process in the near wall region, and that secondary hairpin legs are more agitated and enhance the mesomixing greater than primary legs. The CVP does not apparently participate in the mesomixing in the wake however it greatly enhances the mass transfer between the wake and the flow core region. Reynolds shear stress values decrease with the distance from the tab due to the decrease in the vorticity momentum. Primary hairpin legs also participate to the mass exchange between the tab wake and the near wall region due to the pumping action. Secondary hairpin legs enhance furthermore the mass transfer in this region. These results are consistent with those found by Dong and Meng [3] who showed that higher kinetic energy is observed in the region of primary hairpin legs; however their study did not show the effect of secondary hairpin legs on the mesomixing process.

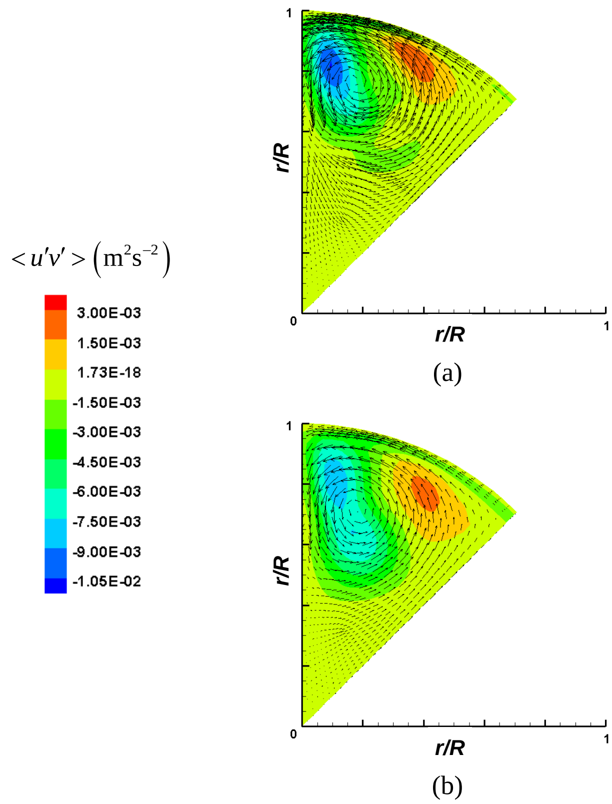

Figure 2. Reynolds shear stress distribution on two cross sections located at (a) *z/h*=0.75 and (b) *z/h*=2.5 downstream from the tab, *Re*= 15000

The mean experimental streamwise velocity radial profiles are plotted in Figure 3 (a) on different cross sections. A great gradient is observed in the mean streamwise velocity profiles at the shear zone $0.4 < y/R < 0.6$, due to the interaction between high momentum fluid in the flow core and low momentum fluid beneath the shear layer shed from the tab. The presence of the primary hairpins is indicated as an inflection point $(\partial^2 W/\partial y^2 = 0)$ (upper inflection points ○). The fitted line coincides with the statistical path of the primary hairpin heads, and shows that they are migrating away from the wall further downstream from the tab. Other inflection points are present below the hairpin heads (lower inflection points ●), and point out the presence of secondary instabilities. PIV measurements by Yang *et al.* [2] and DNS by Dong and Meng [3] showed that these secondary structures have an opposite-signed vorticity relatively to the hairpin heads and convect downstream below the hairpins. These reversed vortices are due to the interaction between the accelerated fluid below a hairpin head and slower fluid further underneath [3,4].

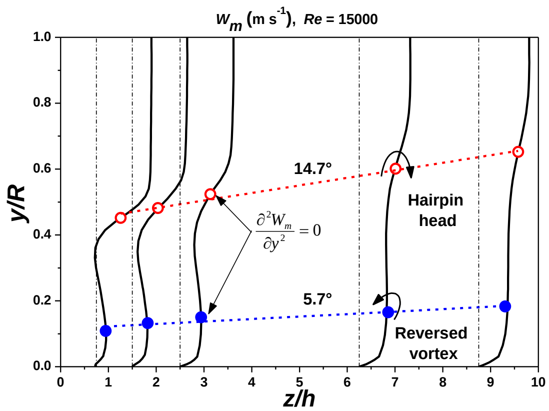

(a)

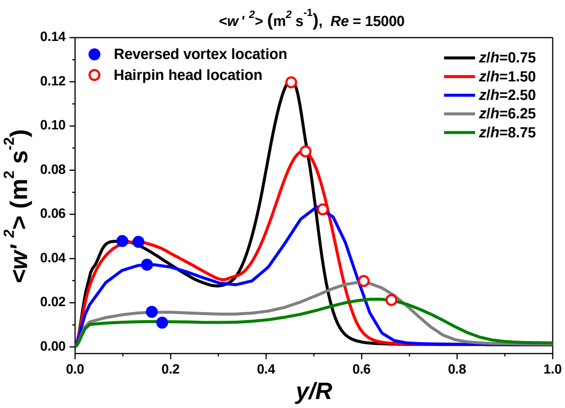

(b)

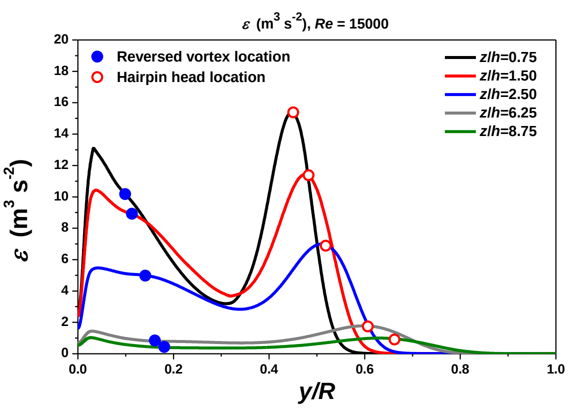

(c)

Figure 3. Experimental radial profiles of the (a) mean streamwise velocity, (b) Reynolds shear stress $< w'^2 >$ and (c) turbulent energy dissipation rate, showing the development of primary hairpin heads (○) and reversed vortices (●) for z/h = 0.75 to 8.75 downstream from the tab, *Re*= 15000.

To analyze the effect of these different structures on turbulent mesomixing, streamwise Reynolds stress $< w'^2 >$ is plotted in Figure 3 (b) for different axial positions downstream from the tab. It is clearly shown that the statistical path of the hairpin heads coincides with the higher pick of $< w'^2 >$ and the statistical path of reversed vortex coincides with the lower pick. This suggests that both primary hairpin heads and reversed vortex participate to the mesomixing in the tab wake (between 1.5 and 3 fold higher). The contribution of the reversed vortices to mesomixing in the region below the hairpins is quickly attenuated between z/h= 2.5 and z/h= 6.25, and the mesomixing due to the primary hairpin heads continuous further downstream from the shear zone, while approaching to the pipe centerline.

In Figure 3 (c) the turbulent energy dissipation rate is represented for different axial positions from the tab. In the present study, the energy dissipation rate is calculated from the following expression, by using Batchelor model [14] based on dimensional analysis:

$$\varepsilon = A \frac{\left(\overline{u^2}\right)^{\frac{3}{2}}}{\Lambda} \tag{1}$$

where Λ represents the scale of the energetic structures, which is the upper limit of the inertial domain in Kolmogorov energy cascades. The value of the A constant is taken at 1,8 (Mokrani *et al.* [12]) and used by Lemenand *et al.* [4] and Mohand Kaci *et al.* [5] for turbulent flow in aligned rows of vortex generators. In the present study, the spatial macroscale is obtained by:

$$\Lambda = \tau U_{conv} \tag{2}$$

with τ the integral time scale given by

$$\tau = \int_0^\infty \frac{\overline{u(t)u(t+T)}}{\overline{u^2(t)}} dT \tag{3}$$

and U_{conv} the convective velocity estimated by Van Doorn [13], and successfully used by Lemenand *et al.* [4] and Mohand Kaci *et al.* [5] for the HEV mixer. Assuming the local isotropy of the turbulence in a one-dimensional mean flow:

$$U_{conv} = U^2\left(1 + 5\frac{\overline{u^2}}{U^2}\right) \tag{4}$$

From the Figure 3 (c), it can be seen that the maximum values of ε coincide with the statistical path of primary hairpin heads, confirming that these structures are responsible for dissipating the turbulent kinetic energy while convecting downstream. The second extremum of ε is located in the near wall region where the production of turbulence is due to the structures present in the wall outer layers intensified by the presence of the CVP common flow that add more fluctuation gradients to the near wall layers. The reversed vortices seem to not contribute to the micromixing process. The heads of hairpin structures transport high momentum fluid from the flow core to the region between hairpin head and reversed vortex, where the fluid is rolled over between these two structures.

In Figure 4 the distribution of Reynolds stress and turbulent energy dissipation fields are represented on a tab plane of symmetry obtained from numerical simulation. From Figure 4 (a), it is verified that high values of Reynolds shear stress observed in Figure 3 (b) coincide with the presence of reversed vortices, as observed by Yang *et al.* [2] and Dong and Meng [4], in the region below the statistical pass of hairpin heads. The maximum values of Reynolds shear stress coincide with the statistical passage of the hairpin heads and persist much farther downstream than the reversed vortices.

From Figure 4 (b), it is observed that the maximum values of the turbulent energy dissipation reflect the statistical path of hairpins heads, which persist in the near tab region, over a distance shorter than for Reynolds shear stress. While convecting downstream, the maximum values of the turbulent energy dissipation decreases with the distance from the tab. The common flow also contributes to the turbulent production for a small distance from the tab as shown in the Figure 4 (b), especially in the zone near the wall.

These observations are in agreement with the experimental results, and put in evidence the contribution of the different flow structures on meso and micromixing.

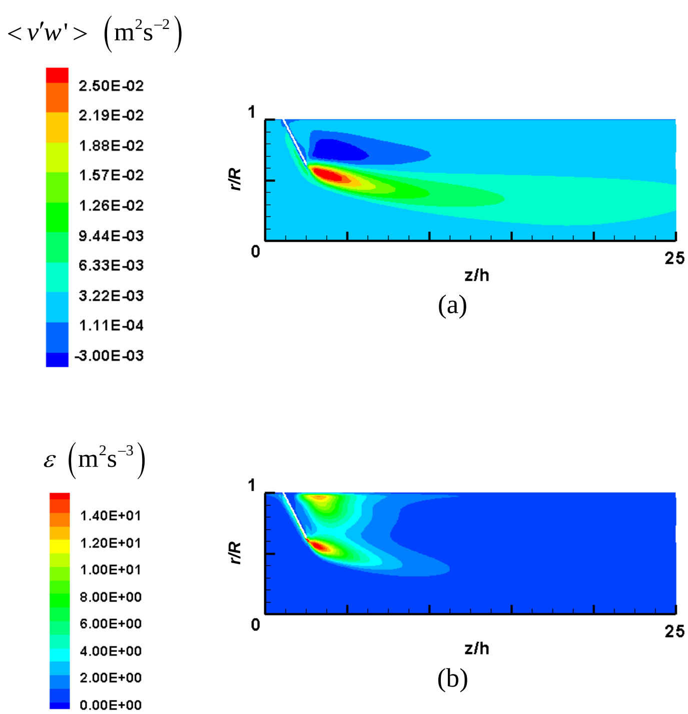

Figure 4. Distribution of (a) Reynolds shear stress and (b) turbulent energy dissipation rate computed in the plane of symmetry of the tabs, for *Re*= 15000

On Figure 5 it can be observed that the maximum values of ε clearly reflect the hairpin head shape (arc of maximum ε in the Figure 5) and complies with the fact that these heads control the micromixing process in the shear region behind the tab. As shown in the Figure 5, the hairpin heads are riding on the top of the CVP, and they are migrating towards the pipe centerline while convecting downstream.

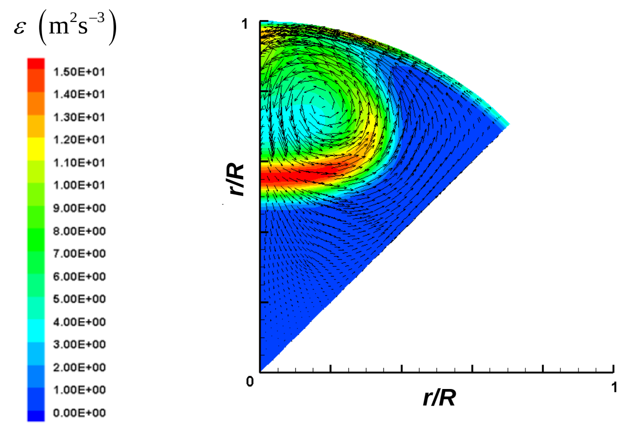

Figure 5. Distribution of the turbulent energy dissipation rate computed on a cross section located at z/h=0.75 downstream from the tabs, for *Re*= 15000

CONCLUSION

The flow past a row of trapezoidal tabs was investigated by using two complementary techniques: LDV measurements and numerical simulations. The flow statistics showed the individual contribution of the different flow structure on meso and micro-mixing. The CVP do not directly participate to meso or micro-mixing process but it plays an essential role in the mass exchange between low momentum fluid near the wall and high momentum fluid in the test section center. However, the common-flow in the tab plan of symmetry created by the CVP increases the velocity fluctuations in the tab wake and enhances the micromixing by increasing the turbulent energy dissipation rate.

Primary and secondary hairpin legs and inversed vortices are the most contributing on both mesomixing downstream from the tab. This fact is identified by maximum values of Reynolds stress tensor which coincide with the statistical path of these instabilities.

Maximum values of turbulence energy dissipation where observed in the region of the primary hairpin heads, leading to conclude that the hairpin heads are the most contributing on micromixing and drop breakup in the shear zone downstream from the tab. Maximum values of turbulent energy dissipation rate are also observed in a short distance downstream from the tab in the near wall region. These high values are due to the interaction of the common flow of the CVP with the low momentum fluid in the wall outer layers. The hairpin legs also contribute to the mass transfer in the tab wake due to the pumping action and fluid ejection from and toward the near wall region. Primary hairpin heads participate to the mass transfer between the tab wake and the flow core, which is further enhanced by the secondary hairpin heads.

The main conclusion is that the understanding of the important role of the hairpin vortices can adjust the tab design promoting these flow structures.

NOMENCLATURE

h	Vortex generator height (m)
I	Turbulence intensity
(u, v, w)	Velocity components (m/s)
(u', v', w')	Fluctuating velocity components (m/s)
W	Mean flow velocity (m/s)
r	Radial coordinate (m)
R	Pipe radius (m)
(x, y, z)	Cartesian coordinates

Greek letters

ε	Turbulent energy dissipation rate (m^2/s^3)
Λ	Scale of the energetic structures (m)
τ	Integral time scale (s)

REFERENCES

[1] Gretta, W.J. and Smith, C.R., The Flow Structure and Statistics of a Passive Mixing Tab, *Trans. ASME J. Fluids Eng.*, Vol. 115, pp. 255-263, 1993.

[2] Yang, W., Meng, H. and Sheng, J., Dynamics of Hairpin Vortices Generated by a Mixing Tab in a Channel Flow, *Exp. Fluids*, Vol. 30, pp. 705-722, 2001.

[3] Dong, D. and Meng, H., Flow Past a Trapezoidal Tab, *J. Fluid Mech.*, Vol. 510, pp. 219-242, 2004.

[4] Lemenand, T., Della Valle, D., Zellouf, Y. and Peerhossaini, H., Droplets Formation in Turbulent Mixing of Two Immiscible Fluids, *Int. J. Multiphase Flow*, Vol. 29, pp. 813-840, 2003.

[5] Mohand Kaci, H., Lemenand, T., Della Valle, D. and Peerhossaini, H., Enhancement of Turbulent Mixing by Embedded Longitudinal Vorticity: a Numerical Study and Experimental Comparison, *Proceedings of ASME FEDSM*, Miami, Florida, July 17-20, 2006, pp. 115-125.

[6] Baldyga, J. and Bourne, J.R., *Turbulent Mixing and Chemical Reactions*, Wiley, Chichester, 1999.

[7] Hinze, J.O., Fundamentals of the hydrodynamic mechanism of splitting in dispersion processes, *AIChE Journal*, Vol. 1, pp. 289-295, 1955.

[8] Launder, B.E. and Spalding, D.B., *Lectures in Mathematical Models of Turbulence*, in Academic Press, London, 1972.

[9] Gibson, M.M. and Launder, B.E., Ground effects on pressure fluctuations in the atmospheric boundary layer, *J. Fluid Mech.*, Vol. 86, pp.491-511, 1978.

[10] Launder, B.E., Reece, G.J. and Rodi, W., Progress in the development of a Reynolds stress turbulence closure, *J. Fluid Mech.*, Vol. 68, pp.537-566, 1975.

[11] Hinze, J.O., *Turbulence*, 2nd ed., McGraw-Hill, New York, 1975.

[12] Mokrani, A., Castelain, C. and Peerhossaini, H., Experimental study of the influence of the rows of vortex generators on turbulence structure in a tube, *Chem. Eng. Proc.*, Vol. 48, pp. 659-671, 2009.

[13] Van Doorn, M., *On Taylor's Hypothesis in Turbulent Shear Flows*, Internal Note 811123, University of Missouri-Rolla, 1981.

[14] Batchelor, G.K., *The Theory of Homogeneous Turbulence*, Cambridge University Press, 1953.